



A method for quantitative analysis of biofilm thickness variability
by Ricardo Murga

A thesis submitted in partial fulfillment of the requirements for the degree of Master of Science in
Environmental Engineering
Montana State University
© Copyright by Ricardo Murga (1994)

Abstract:

This thesis presents work done on developing an experimental method for measurement of biofilm thickness. This method involves embedding the biofilm, cross-sectioning it, and applying image analysis and mathematical techniques to reconstruct biofilm thickness profiles in order to characterize biofilm thickness variation. Quantitative data as well as qualitative observations obtained from *Pseudomonas aeruginosa*, *Klebsiella pneumoniae* and binary population biofilms revealed that the three biofilm systems are distinct and heterogeneous in their structure. Statistical analysis of biofilm thickness data showed that biofilm species composition influences structural characteristics. *P. aeruginosa*, *K. pneumoniae* and binary population biofilms appeared to have different mean thicknesses, different roughness values, and different spatial, distribution of biomass, voids and water channels. *P. aeruginosa* biofilms are relatively uniform and lack voids or water channels. They have an average thickness of 30 μm , and their roughness coefficient, Ra^* , ranges between 0.1 and 0.2. Different sizes and lengths of water channels were observed in *K. pneumoniae* biofilms, but the most distinctive characteristic was large bare areas along the substratum. *K. pneumoniae* biofilms are patchy and their thickness varies drastically, having a mean thickness that ranged between 8 μm to almost 300 μm . The roughness coefficient for *K. pneumoniae* biofilms was the highest of the three biofilms systems, ranging between 0.8 to 1.3. The binary population biofilm was also full of water channels and voids. The mean thickness ranged between 300 and 600 μm , but its roughness coefficient only ranged between 0.2 and 0.3. The different ranges for the roughness coefficient values suggested that differences in biofilm thickness variation could be used as a distinctive characteristic for categorizing biofilms.

A METHOD FOR QUANTITATIVE ANALYSIS OF BIOFILM
THICKNESS VARIABILITY

by
Ricardo Murga

A thesis submitted in partial fulfillment
of the requirements for the degree

of
Master of Science
in
Environmental Engineering

MONTANA STATE UNIVERSITY
Bozeman, Montana

April 1994

7378
m944

APPROVAL

of a thesis submitted by

Ricardo Murga

This thesis has been read by each member of the committee and has been found to be satisfactory regarding content, English usage, format, citations, bibliographic style, and consistency, and is ready for submission to the College of Graduate Studies.

4/27/94
Date

Philip A. Stewart
Chairperson, Graduate Committee

Approved for the Major Department

27 April 1994
Date

Shedice E. Lang
Head, Major Department

Approved for the College of Graduate Studies

5/4/94
Date

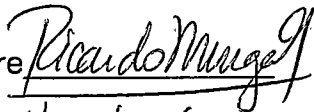
R. L. Brown
Graduate Dean

STATEMENT OF PERMISSION TO USE

In presenting this thesis in partial fulfillment of the requirements for a master's degree at Montana State University, I agree that the Library shall make it available to borrowers under rules of the Library.

If I have indicated my intention to copyright this thesis by including a copyright notice page, copying is allowable only for scholarly purposes, consistent with "fair use" as prescribed in the U.S. Copyright Law. Requests for permission for extended quotation from or reproduction of this thesis in whole or in parts may be granted only by the copyright holder.

Signature



Date

4/27/94

ACKNOWLEDGEMENTS

First I would like to express my gratitude to my academic and research advisor Dr. Phil Stewart. He has provided the support, guidance, and encouragement which have enabled me to accomplish this goal. I also thank my committee members, Dr. Warren Jones for his counsel and assistance during my first semester at MSU, and Dr. Zbigniew Lewandowski for his assistance.

I would like to acknowledge Gayle Callis for the many hours of work and for her advice on further developing biofilm cryoembedding. I would also like to acknowledge Don Daly for his advice and help on the use of statistical tools.

The staff and fellow graduate students at the Center for Biofilms Engineering have been very helpful to me, and have made my stay at the ERC very pleasant. I would like to especially thank for their help Gary, Dirk, Brian, Diane, Peg, Jamie, Paul, and Marty. Many thanks also for their help and friendship to Jason, Xiaoming, Philip, Sam, Mary, Nick, and specially Rohini.

I would like to acknowledge with love and gratitude the support and encouragement of my wife, Jennifer.

My special thanks to Bill Characklis for the existence of the Center, for his great example and vision.

My research activities have been sponsored by the National Science Foundation and the Associates of the Center; my thanks to them.

Most important of all I thank my God for His grace and love for me.

TABLE OF CONTENTS

	Page
LIST OF TABLES	vii
LIST OF FIGURES	viii
ABSTRACT	xi
INTRODUCTION	1
The Problem	1
Goal and Objectives	3
LITERATURE REVIEW	4
Evidence of Biofilm Structural Heterogeneity	4
METHOD DEVELOPMENT	10
MATERIALS, EXPERIMENTAL SYSTEMS AND METHODS	11
Bacterial Characteristics	11
Reactor Design	11
Reactor Start-up	16
Sampling	16
Biofilm Cryoembedding	18
Cryosectioning	19
Fixation and Staining of Biofilm Cross-sections	21
Image Analysis	22
Statistical Methods	23
RESULTS	27
DISCUSSION	64
Biofilm Thickness Measurements	64
Statistical Analysis	66
Biofilm Heterogeneity	68
SUMMARY AND CONCLUSIONS	74
RECOMMENDATIONS FOR FUTURE RESEARCH	77
REFERENCES	79

APPENDICES	86
APPENDIX A	87
Particle Sizing Using Image Analysis Techniques	87
Vernier Measurements	92
Coulter Counter Measurements	95
APPENDIX B	101
Optical Measurements	101
Biofilm Embedding	103
APPENDIX C	109
S-PLUS Program	109

LIST OF TABLES

Table		Page
1.	References for evidence of heterogeneity	5
2.	Medium composition	15
3.	Phosphate buffer composition	15
4.	Coulter Counter aperture tube data	99

LIST OF FIGURES

Figure		Page
1.	Annular reactor schematic	12
2.	Cryoembedding schematic	20
3.	Photomicrographs of the substratum after biofilm remov	32
4.	Photomicrographs of <i>P. aeruginosa</i> biofilm cross-section	33
5.	Photomicrographs of <i>K. pneumoniae</i> biofilm cross-section ...	34
6.	Photomicrographs of binary population biofilm cross-section ..	35
7.	<i>P. aeruginosa</i> biofilm profiles from three different random locations on the slide (a, b and c)	36
8.	<i>K. pneumoniae</i> biofilm profiles from three different random locations on the slide (a, b and c)	37
9.	Binary population biofilm profiles from three different random locations on the slide (a, b and c)	38
10.	<i>P. aeruginosa</i> biofilm thickness distributions from profiles on figures 7a through 7c	39
11.	<i>K. aeruginosa</i> biofilm thickness distributions from profiles on figures 8a through 8c	40
12.	Binary population biofilm thickness distributions from profiles on figures 9a through 9c	41
13.	Variogram curves from <i>P. aeruginosa</i> biofilm profiles on figures 7a through 7c	42
14.	Variogram curves from <i>K. pneumoniae</i> biofilm profiles on figures 8a through 8c	43
15.	Variogram curves from binary population biofilm profiles on figures 9a through 9c	44
16.	Values of Ra* (roughness coefficient) for <i>P. aeruginosa</i> , <i>K.</i> <i>pneumoniae</i> , and binary population biofilms	45

17.	2-day old binary population biofilm profiles from four different random locations on the slide	46
18.	4-day old binary population biofilm profiles from four different random locations on the slide	47
19.	6-day old binary population biofilm profiles from three different random locations on the slide	48
20.	8-day old binary population biofilm profiles from four different random locations on the slide	49
21.	Binary population biofilm thickness distributions from profiles on figures 17a through 17d	50
22.	Binary population biofilm thickness distributions from profiles on figures 18a through 18d	51
23.	Binary population biofilm thickness distributions from profiles on figures 19a through 19c	52
24.	Binary population biofilm thickness distributions from profiles on figures 20a through 20c	53
25.	Variogram curves from profiles on figures 17a through 17d . . .	54
26.	Variogram curves from profiles on figures 18a through 18d . . .	55
27.	Variogram curves from profiles on figures 19a through 19c . . .	56
28.	Variogram curves from profiles on figures 20a through 20c . . .	57
29.	Ra* values from biofilm profiles on figures 17a through 20c . . .	58
30.	Mean biofilm thickness from biofilm profiles on figures 17a through 20c	59
31.	Biofilm density for binary population biofilm 2, 4, 6, 8 days old .	60
32.	Individual cells and multicellular aggregates observed in the effluent of a <i>P. aeruginosa</i> biofilm reactor	61
33.	Multicellular aggregates observed in the effluent of a <i>K. pneumoniae</i> biofilm reactor	62

34.	Individual cells and multicellular aggregates observed in the effluent of a binary population biofilm reactor	63
35.	Relationship between Ra^* and variogram distance for <i>P. aeruginosa</i> , <i>K. pneumoniae</i> and binary biofilms	71
36.	Photomicrographs of undefined mixed population biofilm cross-section	72
37.	Photomicrographs of binary population biofilm cross-section grown with continuous supply of $CaCO_3$ and kaolin	73
38.	Particle area distribution of detached <i>P. aeruginosa</i> multicellular aggregates from days 1 through 4	89
39.	Particle area distribution of detached <i>P. aeruginosa</i> multicellular aggregates collected on hours 1 through 4 of day 5	90
40.	Particle area distribution of detached <i>P. aeruginosa</i> multicellular aggregates collected on hours 5 through 8 of day 5	91
41.	Polar Planimeter	93
42.	Image Analysis and planimeter results comparison	96
43.	Planimeter results from measuring square and circular shapes	97
44.	Method for measuring wet biofilm thickness with an optical microscope	102
45.	<i>P. aeruginosa</i> and <i>K. pneumoniae</i> biofilm thickness profiles	106
46.	Undefined mixed population biofilm thickness profile	108

ABSTRACT

This thesis presents work done on developing an experimental method for measurement of biofilm thickness. This method involves embedding the biofilm, cross-sectioning it, and applying image analysis and mathematical techniques to reconstruct biofilm thickness profiles in order to characterize biofilm thickness variation. Quantitative data as well as qualitative observations obtained from *Pseudomonas aeruginosa*, *Klebsiella pneumoniae* and binary population biofilms revealed that the three biofilm systems are distinct and heterogeneous in their structure. Statistical analysis of biofilm thickness data showed that biofilm species composition influences structural characteristics. *P. aeruginosa*, *K. pneumoniae* and binary population biofilms appeared to have different mean thicknesses, different roughness values, and different spatial distribution of biomass, voids and water channels. *P. aeruginosa* biofilms are relatively uniform and lack voids or water channels. They have an average thickness of 30 μm , and their roughness coefficient, Ra^* , ranges between 0.1 and 0.2. Different sizes and lengths of water channels were observed in *K. pneumoniae* biofilms, but the most distinctive characteristic was large bare areas along the substratum. *K. pneumoniae* biofilms are patchy and their thickness varies drastically, having a mean thickness that ranged between 8 μm to almost 300 μm . The roughness coefficient for *K. pneumoniae* biofilms was the highest of the three biofilms systems, ranging between 0.8 to 1.3. The binary population biofilm was also full of water channels and voids. The mean thickness ranged between 300 and 600 μm , but its roughness coefficient only ranged between 0.2 and 0.3. The different ranges for the roughness coefficient values suggested that differences in biofilm thickness variation could be used as a distinctive characteristic for categorizing biofilms.

INTRODUCTION

The Problem

Microbial cells attach firmly to almost any surface submerged in an aquatic environment. The immobilized cells grow, reproduce, and produce extracellular polymers which help them form a complex matrix that provides structure to the biomass accumulation termed a *biofilm* (Characklis and Marshall, 1990). The adhesion to surfaces provides considerable advantages for bacteria within the biofilm. The biofilm matrix provides protection from antimicrobial agents, as well as facilitating the exchange of nutrients and genetic material due to close proximity of cells. While bacteria benefit from their close association with the surface, the physical presence of the biofilm compromises the function of the surface, reducing the efficiency of equipment in industry. This damage to the surface is referred to as biofouling. Some of the problems stemming from biofouling are summarized in the following paragraph.

Microbially induced corrosion (MIC) is initiated when clusters of bacteria form a patchy biofilm. These clusters establish microscale chemical gradients around the surface and thereby create both anodic and cathodic sites (Lee and Characklis, 1993., Geesey and Bremer, 1992., Videla and Characklis, 1992., Bremer and Geesey, 1991., Characklis et al. 1991, Geesey, 1990., Jelley et al., 1989., Characklis, 1989). Increase of fluid-frictional resistance in industrial

pipes results from the increase in biofilm thickness and roughness (Characklis, Zilver and Turkhia, 1981., Characklis and Turkhia, 1981., Picologlou et al., 1980., Kirkpatrick et al. 1980., Characklis, Zilver and Picologlou, 1978).

Increase of heat transfer resistance results from the accretion of biomass and inorganic sediments (Turakhia and Characklis, 1984., Mussalli and Characklis, 1984., Characklis et al. 1984, 1983., Zilver et al., 1982., Characklis Nimmons and Picologlou, 1981., Characklis, Zilver and Turakhia, 1981). Bacterial colonization of a variety of medical implants and devices results in persistent infections (Costerton, 1982., Marrie et al., 1982., Marrie and Costerton, 1983., Marrie and Costerton, 1984). Detachment of microbial aggregates into the bulk liquid degrades products in the paper manufacturing and water distribution processes (Nix, et al. 1992., Block, 1992., Jung, et al. 1990., McFeters, 1990., van der Wende, et al. 1989., LeChevallier, et al. 1988., Camper, et al. 1986).

Biofilm development and activity is the result of several physical, chemical and biological rate processes. Such processes include transport of cells to the substratum, adsorption of cells onto the substratum, growth and other metabolic processes within the biofilm, and detachment of portions of the biofilm. These processes are influenced by the biofilm structure and the properties of the environment around the biofilm. Surface roughness, for example, significantly influences transport rates and microbial attachment for several reasons including the following: 1) increased convective mass transport near the surface, 2) shelter from shear forces for small particles, and 3)

increased surface area for attachment (Characklis, W.G., 1981). Surface roughness is one of the many aspects that reflect the structural heterogeneity of the biofilm matrix. This structural heterogeneity should therefore be studied and quantitatively described in order to better understand, predict and solve the problems caused by biofouling. Obtaining quantitative information on surface roughness and structural heterogeneity remains a challenge to biofilm researchers.

Goal and Objectives

The long term goal of this research is to understand how biofilm structural heterogeneity impacts biofilm function. The broad objective of this thesis was to develop experimental methods and apply mathematical techniques to characterize biofilm thickness variation. The specific objectives were: 1) to develop an experimental method suitable for measurement of biofilm thickness profiles, 2) to construct 1-dimensional thickness profiles of steady state pure culture biofilms of *P. aeruginosa*, *K. pneumoniae*, and the binary population combination, 3) to calculate a roughness index (R_a^*) and to perform a spatial correlation analysis for each profile, 4) to obtain photomicrographs of particles in the effluent of pure culture and binary population biofilm reactors, 5) to document temporal changes in biofilm thickness characteristics during development of binary population biofilms by obtaining biofilm thickness profiles, R_a^* values, and spatial correlation analyses in time series.

LITERATURE REVIEW

Evidence of Biofilm Structural Heterogeneity

Recent publications provide evidence of structural heterogeneity in biofilms. Table 1 shows a few examples of the types of evidence described in publications from the last decade alone. Several techniques have been used to qualitatively describe biofilm structure including light microscopy, atomic force microscopy (AFM), scanning electron microscopy (SEM), transmission electron microscopy (TEM), confocal scanning laser microscopy (CSLM), and Fourier transmission infrared spectroscopy (FTIR). The systems in which these observations were made range from laboratory reactors to medical and industrial systems.

Many factors may contribute to the structural heterogeneity of biofilms such as the uneven distribution of microbial species, the presence of different shapes of bacteria buried in amorphous extracellular polymers that constitute the biofilm matrix, nitrogen bubble formation in some cases, shear and hydrodynamic forces, deposits of sediments, and encrustations on pipe walls. All these contribute to different forms of structural heterogeneity in biofilms due to the disruption of the microbial matrix and biomass detachment (sometimes leaving entire bare areas), helping to the formation of patchy biofilms. Most heterogeneous biofilms have water channels, pores, microtowers, ridges, and large variations in biofilm thickness and surface roughness.

Table 1. References for evidence of heterogeneity.

Author	Ref	Microorganism	Reactor Design	Evidence
Allen et al, 1980.	1	Mixed population.	Wat. dist. system	Electron micrographs revealed a hard but porous surface.
Bremer et al, 1992.	7	CCI#8 bacterium.	Copper coupons submerged in flasks with culture medium.	Atomic Force Microscopy (AFM) showed biofilm "several cells thick in places, distributed heterogeneously over coupon surface with considerable variation in surface contour.
Bryers, 1991.	9	<i>P. putida</i> .	Annular reactor.	Observed sloughing events due to nitrogen bubble formation that lead to disruption of the microbial matrix.
Bryers and Characklis, 1981.	10	Undefined mixed population from sewage.	Tubular reactor system running as CSTR	Microscopically, biofilms appeared as discrete fibers randomly distributed, 1.5 to 1500 μm long.
Capdeville et al, 1990.	12	Heterotrophes.	Annular reactor	SEM and photographs showed observations of thickness profile and top view of rough, filamentous and patchy surface.
Christensen et al, 1988.	24	Denitrifying biofilm from wastewater.	Annular reactor	Pictures show heterogeneity in biofilm accumulation due to nitrogen bubble formation.

Table 1 (cont.)

Eighmy et al, 1983.	29	Undefined biofilm from wastewater.	Inert substratum and supporting structure suitable for submersion in wastewater, bacterial adhesion and subsequent examination by TEM and SEM.	SEM and TEM micrographs showed filamentous non-smooth surface.
Gujer, 1987.	34		A model of segregation of biomass in biofilms.	Describes a biofilm as an inhomogeneous microbial matrix due to uneven distributions of microbial species.
Hamoda and Abd-el-bary, 1987.	35	Mixed culture from activated sludge.	Aerated submerged fixed-film (ASFF) bioreactor.	Microscopic observation of spongy biofilms with thickness of up to 2.3 mm.
Harremoes et al, 1980.	37	Denitrifying biofilm.	Annular reactor.	Extreme heterogeneity in biofilms due to nitrogen bubbles formation that detached big particles of biofilm leaving large bare sections of the wall visible.
Howell and Atkinson, 1976.	38		Trickling filter biofilm model.	Computer output showed film thickness profiles to have a varied irregular pattern.

